Buckling, Postbuckling, and Failure of Stiffened Panels Under Shear and Compression

Rocky R. Arnold* and Jatin C. Parekh†
Anamet Laboratories, Inc., Hayward, California

A theoretical/analytical capability for prediction of buckling, postbuckling, and failure of flat and shallow-curved, edge-stiffened laminated composite plates under combined axial compression and shear is discussed. The initial buckling predictions are based on linear elasticity; however, the postbuckling calculations include the material nonlinearity present in the composite. Specifically, three in-plane Ramberg-Osgood stress-strain relations are used to describe the laminae and the matrix material between laminae is modeled with one Ramberg-Osgood relationship for transverse shear. Accurate representations of stress and strain distributions permit comparison to material allowables; thus, failure predictions can be made.

Nomenclature

A_s = stiffener cross-sectional area
$a_{ij}, b_{ij}, \ldots$ = arbitrary interlaminar shear coefficients
b = stiffener spacing
D_{ij}, D = bending stiffnesses from classical lamination theory with $D \equiv D_{22}$
e_{ij}, f_{ij}, g_i = arbitrary displacement coefficients
G_s = average shear modulus of stiffener
h, t = laminate thickness
h_{pij} = arbitrary membrane and bending stress coefficients
J_s = stiffener equivalent torsional rigidity
L = plate length
m = number of half-buckle wavelengths in x direction
n = number of half-buckle wavelengths in y direction
$N_x, N_{x_{cr}}, N_{x_{cr_p}}$ = average axial load, buckling load in compression for panel, and simply supported orthotropic flat panel, respectively
$N_{xy}, N_{xy_{cr}}, N_{xy_{cr_p}}$ = average shear load, buckling load in shear for panel, and simply supported orthotropic flat panel, respectively
R = panel radius
$S_{x_k}^{(0)}, S_{x_k}^{(1)}, \ldots$ = stiffness ratio factors as defined in Ref. 50
u_k, v_k = median surface inplane displacements of kth lamina
w = lateral displacement function
x, y, z = plate coordinates, see Fig. 1
Z = nondimensional curvature parameter, $= (b^2/Rt)\sqrt{1-\nu^2}$
α = slope of nodal lines in buckled waveform
δ, δ_{cr_p} = applied unit and critical end shortening for a flat plate, respectively
Ω, Ω_{cr_p} = applied unit and critical shear strain for a flat plate, respectively
τ_s = average torsional shear stress in stiffener
τ_{xy_k} = median surface shearing stress of the kth lamina
τ_{yz_k}, τ_{zx_k} = interlaminar shearing stresses of kth matrix layer

Subscripts

e = linear-elastic materials
k = kth lamina
p = nonlinear-elastic materials

Presented as Paper 86-1027 at the AIAA/ASME/ASCE/AHS 27th Structures, Structural Dynamics and Materials Conference, San Antonio, TX, May 19–21, 1986; received July 24, 1986; revision received April 4, 1987.

*Principal Engineer. Member AIAA.
†Engineer

Introduction

STIFFENED-PANEL structures are the basic building blocks of most aircraft and helicopter structures. Various missile and spacecraft structures also use an efficient proportioning of discrete stiffening members to increase the overall strength of the panel. Thus, it is not too surprising that the problems associated with the buckling, postbuckling, and maximum strength of stiffened panels have received a great deal of attention over the years. In the following paragraphs, a brief review of the literature related to the shearing of plates is provided so as to place the current effort in the proper historical perspective.

Timoshenko presented the first approximate solution for the symmetric shear buckling of flat isotropic plates[1] (later included in his classic text on elastic stability[2]). However, the exact solution for the shear buckling of a simply supported long isotropic plate was provided by Southwell and Skan.[3] Later, Seydel[4] examined the shear buckling of long orthotropic plates with simply supported and clamped boundary conditions based in part on the earlier work of Bergmann and Reissner.[5] Bollenrath[6] provided a more complete review of theoretical and experimental work conducted prior to 1930.

The problem of shear buckling for panels with curvature was initially examined by Leggett[7]; however, his numerical computations were valid only for panels with small curvatures. Later, Kromm[8] investigated the shear buckling of long panels with constant curvature and moment-free edges under combined shear and axial stresses using an energy approach and the Ritz method, which provided a relatively simple solution process.

Investigations into the behavior of flat isotropic plates with elastic restraints against rotation along the long sides were presented by Stowell and Schwartz[9,10] based upon an extension of the work of Southwell and Skan.[3] Batdorf and Houbolt[11] provided solutions for long plates loaded with shear and transverse compression and concluded that the interaction equation for shear and axial compression[9] ($r_s^2 + r_c = 1$) is conservative when applied to the problem of shear and transverse compression. Using an energy approach, Stein and Neff[12] examined both symmetric and antisymmetric buckling modes and showed that, for certain values of the plate aspect ratio, the antisymmetric buckling load is lower than the symmetric value calculated by Timoshenko.[2] By considering 10 terms in the deflection function for out-of-plane displacements, Batdorf and Stein[13] provided accurate solutions for plates with shear and either axial or transverse loads. Using the Galerkin method to solve the differential equations of equilibrium, Batdorf et al.[14,15] presented solutions for curved plates with various boundary conditions covering a complete range of curvature. Clamped, rectangular plates in shear have been investigated by Southwell and Skan,[3] Cox,[16] Iguchi,[17] and Smith[18] for an assumed symmetrical buckle pattern; however, Budiansky and Connor,[19] using the Lagrangian multiplier method,[20] considered both symmetric and antisymmetric buckle patterns and provided comparisons to show the differences between the various cited references. A semiempirical method for the shear buckling of finite-length panels with substantial curvature causing a sensitivity to imperfections is described by Schildcrout and Stein.[21] This particular document presents design curves which were extensively used in the design guide books written by Gerard and Becker[22] and Bruhn.[23]

Plates with transverse stiffeners loaded in shear were treated by Stein and Fralich[24]; their paper contains additional references pertaining to shear buckling of stiffened panels. However, their investigations considered only the bending stiffness of the stiffener. Later investigations by Rockey and Cook[25] examined the effects of the torsional stiffness of the stiffener on the shear buckling of flat panels.

Approximate formulas for the stability of long plates made of multilayered plywood strips under shearing forces, according to Lekhnitskii,[26] were first presented by Balabukh.[27] Classical solutions for the buckling of flat anisotropic plates under shear and combined shear and compression were also obtained by Lekhnitskii.[26] Recently, using various theoretical approaches, several buckling analyses[28–31] have been made for generally laminated plates under various loading conditions. Viswanathan et al.[28] obtained solutions for laminated, curved, long rectangular plates subjected to combined loads. Sawyer[29] analyzed the compression and shear buckling of finite-length, simply supported composite plates. Using different solution techniques, Zhang and Matthews[30] and Whitney[31] analyzed the buckling of laminated, curved plates under combinations of axial compression and in-plane shear. A comprehensive review of the buckling of laminated composite plates and shells has recently been provided by Leissa.[32]

For panels that must operate with a significant postbuckling strength, the available theoretical approaches are much more limited than those that apply to just initial buckling. Bouadi[33] and Giaedi[34] have used Reissner's variational principle to determine buckling and postbuckling characteristics of square and long simply supported flat unstiffened composite plates under combined compression and shear loadings. Feng[35] analyzed the postbuckling of flat stiffened rectangular panels under compression and shear loadings using an energy approach. Stein[36] studied the postbuckling behavior of long orthotropic plates in combined shear and compression by solving the nonlinear large-deflection partial differential equations of von Kármán. Recently, Zhang and Matthews[37] presented solutions for the postbuckling of unstiffened simply supported, laminated, anisotropic, curved plates under combined axial compression and in-plane shear.

With respect to prediction of the ultimate load capability of postbuckled panels in shear or in combined compression and shear, the available technology is primarily experimental in nature. The experimental studies of Refs. 38–44 are directed toward the problem of quantifying the postbuckling and failure behavior of composite plates under shear loading in the absence of a well-founded predictive capability.

The present paper presents a solution valid for flat or curved, edge-stiffened, anisotropic, laminated composite plates (Fig. 1) under either compression, shear, or combined compression and shear loads based upon the theoretical approach described in Refs. 45–48. The nature of the formulation is such that initial buckling and postbuckling stiffnesses are accurately predictable within the context of a general nonlinear material and kinematic model that uses the Reissner variational principle.[49]

Method of Solution

Once the Reissner functional is constructed, as described in Ref. 48, the appropriate displacement and stress functions, outlined in the following equations, are chosen to effect a solution.

$$
\begin{aligned}
u_k = {} & -\delta x + \Omega y + e_{11} \sin\frac{2\pi m}{L}(x - \alpha y) \cos\frac{2\pi n y}{b} \\
& + e_{12} \cos\frac{2\pi m}{L}(x - \alpha y) \sin\frac{2\pi n y}{b} \\
& + e_{13} \cos\frac{2\pi m}{L}(x - \alpha y) + e_{14} x \\
& + e_{15} \cos\frac{2\pi m}{L}(x - \alpha y) \cos\frac{2\pi n y}{b} \\
& + \left(\frac{z_k}{h}\right)\left[e_{21} \sin\frac{m\pi}{L}(x - \alpha y) \cos\frac{n\pi y}{b} \right. \\
& + e_{22} \sin\frac{pm\pi}{L}(x - \alpha y) \cos\frac{qn\pi y}{b} \\
& \left. + e_{23} \sin\frac{m\pi}{L}(x - \alpha y)\left(1 + \cos\frac{2n\pi y}{b}\right)\right]
\end{aligned} \tag{1}
$$

$$
\begin{aligned}
V_k = {} & f_{11} y + f_{12} \cos\frac{2\pi m}{L}(x - \alpha y) \sin\frac{2\pi n y}{b} \\
& + f_{13} \sin\frac{2\pi m}{L}(x - \alpha y) \cos\frac{2\pi n y}{b} \\
& + f_{14} \sin\frac{2\pi m}{L}(x - \alpha y) \sin\frac{2\pi n y}{b} \\
& + \left(\frac{z_k}{h}\right)\left\{ f_{21}\left[\cos\frac{m\pi}{L}(x - \alpha y) \sin\frac{n\pi y}{b} \right.\right. \\
& \left. - \alpha\beta \sin\frac{m\pi}{L}(x - \alpha y) \cos\frac{n\pi y}{b} \right] \\
& + f_{22}\left[\cos\frac{pm\pi}{L}(x - \alpha y) \sin\frac{qn\pi y}{b} \right. \\
& \left. - \alpha\beta\frac{p}{q} \sin\frac{pm\pi}{L}(x - \alpha y) \cos\frac{qn\pi y}{b} \right] \\
& + f_{23}\left[\cos\frac{m\pi}{L}(x - \alpha y) \sin\frac{2n\pi y}{b} \right. \\
& \left.\left. - \frac{1}{2}\alpha\beta \sin\frac{m\pi}{L}(x - \alpha y)\left(1 + \cos\frac{2n\pi y}{b}\right)\right] + f_{24} \sin\frac{n\pi y}{b} \right\}
\end{aligned} \tag{2}
$$

$$
\begin{aligned}
w = {} & g_1 \cos\frac{m\pi}{L}(x - \alpha y) \cos\frac{n\pi y}{b} \\
& + g_2 \cos\frac{pm\pi}{L}(x - \alpha y) \cos\frac{qn\pi y}{b} \\
& + g_3 \cos\frac{m\pi}{L}(x - \alpha y)\left(1 + \cos\frac{2n\pi y}{b}\right) + g_4 \cos\frac{n\pi y}{b}
\end{aligned} \tag{3}
$$

$$
\begin{aligned}
\sigma_{x_k} = S_{x_k}^{(0)}\Bigg[& h_{111} + h_{112}\cos\frac{2n\pi y}{b} \\
& + h_{113}\sin\frac{2m\pi}{L}(x-\alpha y) \\
& + h_{114}\cos\frac{2m\pi}{L}(x-\alpha y)\cos\frac{2n\pi y}{b} \\
& + h_{115}\sin\frac{2m\pi}{L}(x-\alpha y)\sin\frac{2n\pi y}{b} \\
& + h_{116}\sin\frac{2m\pi}{L}(x-\alpha y)\cos\frac{2n\pi y}{b}\Bigg] \\
& + S_{x_k}^{(1)}\left(\frac{z_k}{h}\right)\Bigg\{h_{121}\Bigg[\cos\frac{m\pi}{L}(x-\alpha y)\cos\frac{n\pi y}{b} \\
& + \alpha\beta\sin\frac{m\pi}{L}(x-\alpha y)\sin\frac{n\pi y}{b}\Bigg] \\
& + h_{122}\Bigg[\cos\frac{pm\pi}{L}(x-\alpha y)\cos\frac{qn\pi y}{b} \\
& + \alpha\beta\frac{p}{q}\sin\frac{pm\pi}{L}(x-\alpha y)\sin\frac{qn\pi y}{b}\Bigg] \\
& + h_{123}\Bigg[\cos\frac{m\pi}{L}(x-\alpha y)\cos\frac{2n\pi y}{b} \\
& + \frac{1}{2}\alpha\beta\frac{p}{q}\sin\frac{m\pi}{L}(x-\alpha y)\sin\frac{2n\pi y}{b}\Bigg] \\
& + h_{124}\Bigg[\cos\frac{m\pi}{L}(x-\alpha y) + \alpha\beta\sin\frac{m\pi}{L}(x-\alpha y)\Bigg]\Bigg\}
\end{aligned}
\tag{4}
$$

$$
\begin{aligned}
\sigma_{y_k} = S_{y_k}^{(0)}\Bigg[& h_{211} + h_{212}\sin\frac{2m\pi}{L}(x-\alpha y) \\
& + h_{123}\cos\frac{2m\pi}{L}(x-\alpha y)\cos\frac{2n\pi y}{b} \\
& + h_{214}\sin\frac{2m\pi}{L}(x-\alpha y)\sin\frac{2n\pi y}{b} \\
& + h_{215}\sin\frac{2m\pi}{L}(x-\alpha y)\cos\frac{2n\pi y}{b}\Bigg] \\
& + S_{y_k}^{(1)}\left(\frac{z_k}{h}\right)\Bigg\{h_{221}\Bigg[(1+\alpha^2\beta^2)\cos\frac{m\pi}{L}(x-\alpha y)\cos\frac{n\pi y}{b} \\
& + 2\alpha\beta\sin\frac{m\pi x}{L}(x-\alpha y)\sin\frac{n\pi y}{b}\Bigg] \\
& + h_{222}\Bigg[\left(1+\frac{p}{q}\alpha^2\beta^2\right)\cos\frac{pm\pi}{L}(x-\alpha y)\cos\frac{qn\pi y}{b} \\
& + \left(\frac{2p}{q}\alpha\beta\right)\sin\frac{pm\pi}{L}(x-\alpha y)\sin\frac{qn\pi y}{b}\Bigg] \\
& + h_{223}\Bigg[\left(1+\frac{1}{4}\alpha^2\beta^2\right)\cos\frac{m\pi}{L}(x-\alpha y)\cos\frac{2n\pi y}{b} \\
& + \alpha\beta\sin\frac{m\pi}{L}(x-\alpha y)\sin\frac{2n\pi y}{b} \\
& + \frac{1}{4}\alpha^2\beta^2\cos\frac{m\pi}{L}(x-\alpha y)\Bigg] \\
& + h_{224}\cos\frac{m\pi}{L}(x-\alpha y) + h_{225}\cos\frac{n\pi y}{b}\Bigg\}
\end{aligned}
\tag{5}
$$

$$
\begin{aligned}
\tau_{xy_k} = S_{xy_k}^{(0)}\Bigg[& h_{311} + h_{312}\sin\frac{2m\pi}{L}(x-\alpha y) \\
& + h_{313}\cos\frac{2m\pi}{L}(x-\alpha y)\cos\frac{2n\pi y}{b} \\
& + h_{314}\sin\frac{2m\pi}{L}(x-\alpha y)\sin\frac{2n\pi y}{b} \\
& + h_{315}\cos\frac{2m\pi}{L}(x-\alpha y)\sin\frac{2n\pi y}{b}\Bigg] \\
& + S_{xy_k}^{(1)}\left(\frac{z_k}{h}\right)\Bigg\{h_{321}\Bigg[\sin\frac{m\pi}{L}(x-\alpha y)\sin\frac{n\pi y}{b} \\
& + \alpha\beta\cos\frac{m\pi}{L}(x-\alpha y)\cos\frac{n\pi y}{b}\Bigg] \\
& + h_{322}\Bigg[\sin\frac{pm\pi}{L}(x-\alpha y)\sin\frac{qn\pi y}{b} \\
& + \frac{p}{q}\alpha\beta\cos\frac{pm\pi}{L}(x-\alpha y)\cos\frac{qn\pi y}{b}\Bigg] \\
& + h_{323}\Bigg[\sin\frac{m\pi}{L}(x-\alpha y)\sin\frac{2n\pi y}{b} \\
& + \frac{1}{2}\alpha\beta\cos\frac{m\pi}{L}(x-\alpha y)\left(1+\cos\frac{2n\pi y}{b}\right)\Bigg] + h_{324}\sin\frac{n\pi y}{b}\Bigg\}
\end{aligned}
\tag{6}
$$

$$
\begin{aligned}
\tau_{yz_k} = \left(\frac{z_k}{n}\right)\Bigg[& b_{11}\sin\frac{m\pi}{L}(x-\alpha y)\cos\frac{n\pi y}{b} \\
& + b_{12}\sin\frac{pm\pi}{L}(x-\alpha y)\cos\frac{qn\pi y}{b} \\
& + b_{13}\sin\frac{m\pi}{L}(x-\alpha y)\left(1+\cos\frac{2n\pi y}{b}\right)\Bigg]
\end{aligned}
\tag{7}
$$

$$
\begin{aligned}
\tau_{xz_k} = \left(\frac{z_k}{n}\right)\Bigg\{ & a_{11}\Bigg[\cos\frac{m\pi}{L}(x-\alpha y)\sin\frac{n\pi y}{b} \\
& - \alpha\beta\sin\frac{m\pi}{L}(x-\alpha y)\cos\frac{n\pi y}{b}\Bigg] \\
& + a_{12}\Bigg[\cos\frac{pm\pi}{L}(x-\alpha y)\sin\frac{qn\pi y}{b} \\
& - \frac{p}{q}\alpha\beta\sin\frac{pm\pi}{L}(x-\alpha y)\cos\frac{qn\pi y}{b}\Bigg] \\
& + a_{13}\Bigg[\cos\frac{m\pi}{L}(x-\alpha y)\sin\frac{2n\pi y}{b} \\
& - \frac{1}{2}\alpha\beta\sin\frac{m\pi}{L}(x-\alpha y)\left(1+\cos\frac{2n\pi y}{b}\right)\Bigg] + a_{14}\sin\frac{n\pi y}{b}\Bigg\}
\end{aligned}
\tag{8}
$$

$$\sigma_s = h_{41} \tag{9}$$

$$\tau_s = h_{61}\frac{mb}{L}\sin\frac{m\pi}{L}(x-\alpha y) \tag{10}$$

These functions are based, in part, on the earlier work of Yoo[45] concerning the effects of curvature on plate maximum strength, Bouadi[33] who demonstrated that Timoshenko's functions[2] can be applied to combined loads, and Arnold and Mayers.[47] The membrane and bending stiffness ratio factors ($S_{x_k}^{(0)}, S_{x_k}^{(1)}, \ldots$), originally derived in Ref. 50, relate laminae stresses to average laminate stresses.

To effect the various inplane boundary conditions, the coefficients e_{14}, f_{11}, f_{12}, and f_{13} are either zero or variationally unknown based upon the chosen in-plane boundary conditions.

Results and Discussion

The results of employing the assumed displacement and stress functions in the previously described theoretical approach are presented in three parts: buckling, postbuckling, and failure. When actual experimental data are available, comparisons to that data will be shown. For the most part, however, data on composite curved panels in combined compression and shear are either not available or are presented in a form that does not allow meaningful comparisons. Consequently, representative values of curvature and edge stiffening are used to describe the results of the analyses. The principal emphasis of this paper is to demonstrate that the selected displacement and stress functions can predict the buckling and postbuckling response of panels loaded in shear and combined compression and shear. Results for axial compression alone have been compared to both experimental data and classical theories and are in essential agreement.[45,47,48] Consequently, load-shortening curves for axial compression have been omitted here.

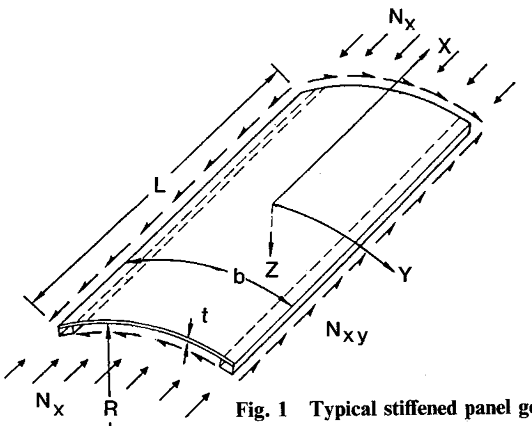

Fig. 1 Typical stiffened panel geometry and applied loads.

Buckling

For curved orthotropic plates, representative trends are shown in Fig. 2 with $\nu \equiv \nu_{12}$, the principal Poisson's ratio. The shear buckling load for plates with curvature and various amounts of edge stiffening has been normalized by the shear buckling load for the analogous flat unstiffened plate. Results for isotropic plates, not shown, are in close agreement to those of Ref. 14.

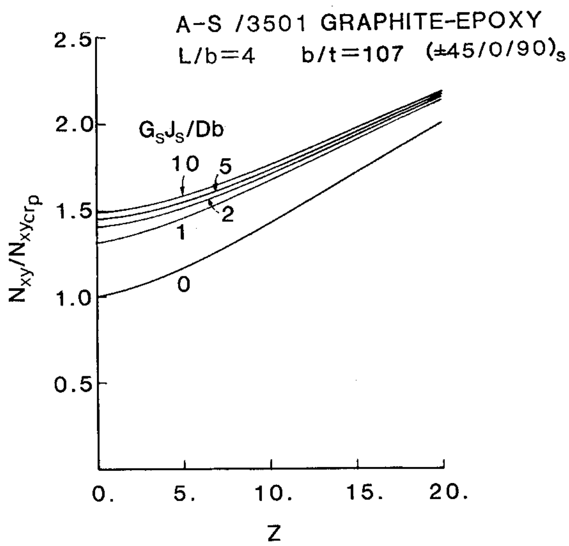

Fig. 2 Effect of curvature and edge stiffening on the shear buckling of long plates.

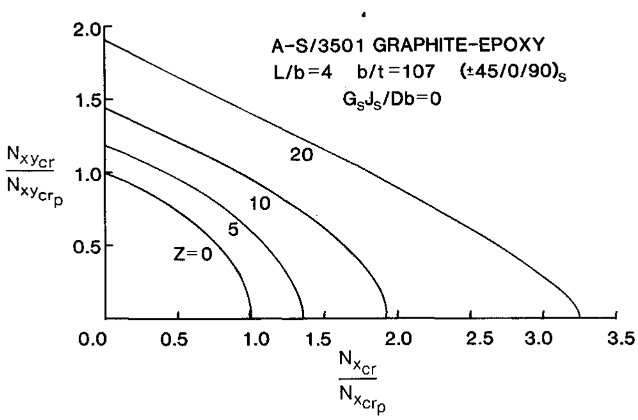

Fig. 3 Effect of curvature on the buckling of composite plates under combined compression and shear.

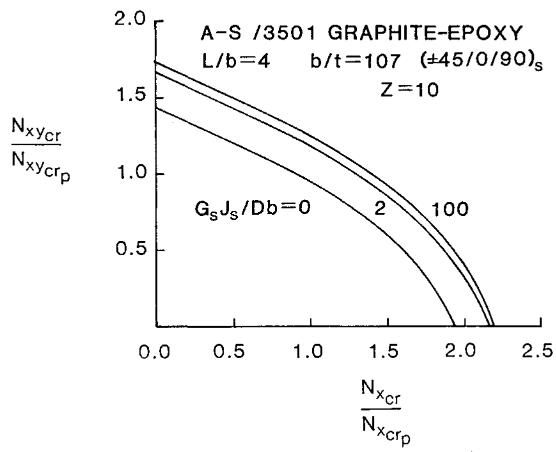

Fig. 4 Effect of edge stiffening on the buckling of composite plates under combined compression and shear.

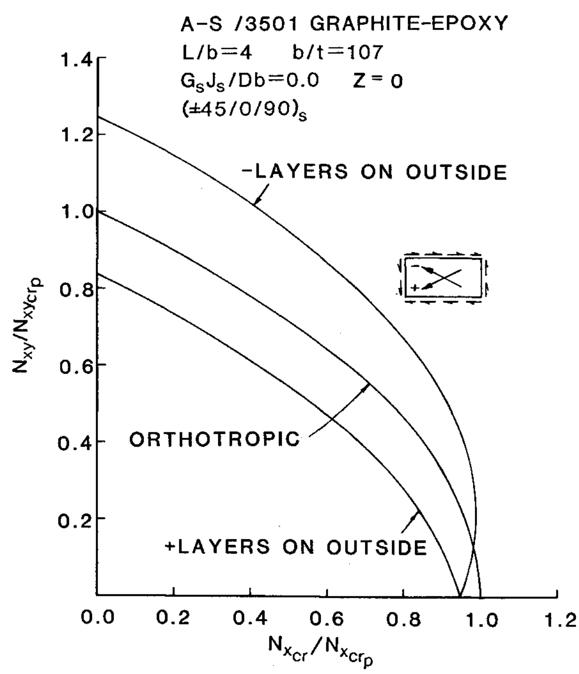

Fig. 5 Effect of anisotropy on the buckling of composite plates under combined compression and shear.

Table 1 Comparison of predicted and experimentally determined initial buckling of flat plates in shear

Panel identification	Material	Layup	L/b	No. of tests	Experimental lb/in.	(kN/m)	Analysis lb/in.	(kN/m)
GDC[44]	A-S/3501	$(\pm 45/0/90)_s$	4.2	1	125	(21.9)	135	(23.6)
Anamet[a]	T300/5208	$(0/\pm 45/90)_s$	2.7	1	116	(20.3)	116	(20.3)
McAir[43]	A-S/3501	$(\pm 45/0/90/0/\pm 45/_T$	5.1	12	102[b]	(17.9)	100	(17.5)
Lockheed[41]	T300/5208	$(\pm 45/90/0/90/\pm 45)_T$	3.3	3	93[b]	(16.3)	95	(16.6)

[a]Source of data proprietary. [b]Average of experimental tests.

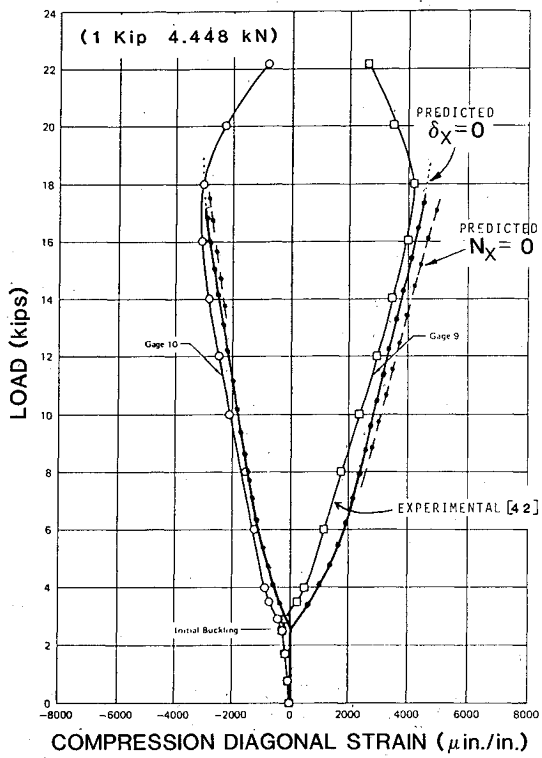

Fig. 6 Correlation of predicted and experimentally determined compression diagonal strain for an edge-stiffened flat panel in shear.

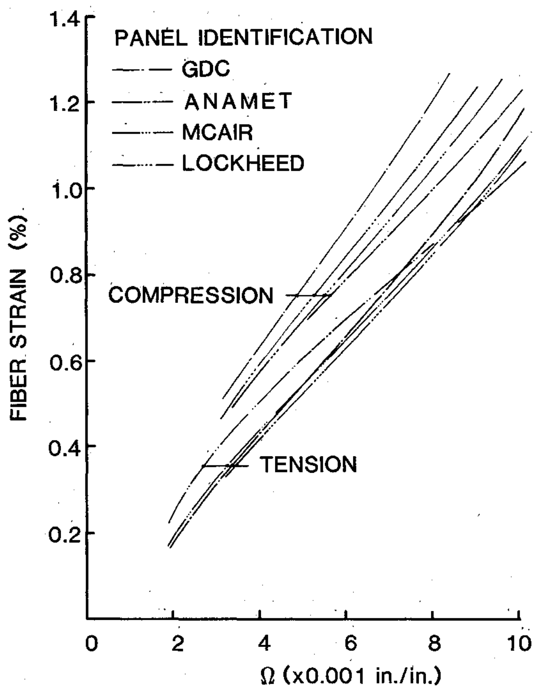

Fig. 7 Fiber strain in edge-stiffened flat panels in shear.

For combined compression and shear, interaction curves for graphite/epoxy laminates are shown in Figs. 3–5. Figure 3 shows the effect of curvature Z on the critical combination of axial compression and shear for an unstiffened panel. The effect of edge stiffening (G_sJ_s/Db) is shown in Fig. 4 for a slightly curved ($Z = 10$) panel. Anisotropy in the panel due to the presence of the D_{16} and D_{26} terms has a distinct effect on initial buckling. Figure 5 shows how bending anisotropy changes the initial buckling loads. Notice that by changing the direction of the outside layers relative to the applied shear stress, the signs of the D_{16} and D_{26} terms are also changed. Clearly, for a flat plate, bending anisotropy has no effect when the load is purely axial compression; however, in pure shear, the bending anisotropy has a very distinct and significant effect on initial buckling because of the direction of the applied shear relative to the minimum/maximum plate stiffnesses (D_{16},D_{26}).

Postbuckling of Flat Panels in Shear

For stiffened flat composite panels loaded in shear, there are several documented experimental test programs[38–44] that provide data on shear buckling, postbuckling, and failure. For convenience, some of these are identified in the following sequence of figures and tables as GDC,[44] Anamet, McAir,[43] and Lockheed,[41] representing tests performed by General Dynamics Convair, Anamet Laboratories, McDonnell Aircraft, and Lockheed Corporation, respectively. The panel identified as Anamet represents an analysis performed on an experimental panel for which most of the data and source are proprietary to a major airframe manufacturer. Each of these panels has been analyzed and typical results are shown. Materials and lamination details are described in Table 1. The predicted initial buckling loads are also compared to the experimental values as shown in Table 1. All panels were designed to have approximately the same initial buckling load of 100 lb/in. (17.51 kN/m). The experimentally obtained load-shortening curves for the McAir, Lockheed, and Anamet panels were not obtained (or the data were not presented); however, experimental data from the GDC panel are in very close agreement with the prediction using inelastic materials. As further evidence of this agreement and to illustrate how strains are accurately predicted by the chosen displacement and stress functions, Fig. 6 shows a comparison of the predicted and experimentally obtained compression diagonal strains for the McAir test specimen. The predicted fiber strains for each of the panels is shown in Fig. 7 as a function of the applied shear strain. In all cases, the compression fiber strain is larger than the tensile fiber strain.

For panels utilizing an adhesively bonded stiffener to provide a load path for shear and compression, the most common failure mode is stiffener disbonding. Using the average torsional stress in the stiffener to calculate the disbonding stress normal to the panel surface, Fig. 8 shows the bondline normal stress as a function of the applied shear strain for each of the experimental panels. The effect of either a linear or a nonlinear elastic material assumption is also seen to have an impact on the magnitude of the bondline normal stress.

Table 2 Comparison of predicted and experimentally determined failure loads of flat panels in shear, lb/in. (kN/m)

	Theoretical predictions					Experimental results			
	Panel crippling[a]		Stiffener disbonding[b]				Failure load		
Panel identification	Tension	Compression	Initial	Final	Failure mode[c]	Stiffener/frame load[d]	Initial	Final[e]	Failure mode[c]
GDC[44]	800 (140.1)	680 (119.1)	410 (71.8)	450 (78.8)	D	0	440 (77.0)	480 (84.0)	D
Anamet[f]	1020 (178.6)	910 (159.3)	N/A[g]	N/A[g]	C	320 (56.0)	1470 (257.4)	1470 (257.4)	C
McAir[43]	700 (122.6)	630 (110.3)	570 (99.8)	630 (110.3)	D	80 (14.0)	620 (108.6)	750 (131.3)	D
Lockheed[41]	650 (113.8)	570 (99.8)	500 (87.6)	550 (96.3)	D	80 (14.0)	470 (82.3)	560 (98.1)	D

[a]Predictions based on fiber strain allowables: $\varepsilon_f = 1.3\%$ (tension), 1.1% (compression). [b]Predictions based on bondline normal stress allowables: 33 psi (227.5 kPa) initial, 36 psi (248.2 kPa) final. [c]Stiffener disbonding (D) or panel crippling (C). [d]Estimated from finite-element analysis and hand calculations. [e]Determined by subtracting estimated stiffener/frame load from experimentally determined total load. [g]Analysis performed in an experimental panel (source of data is proprietary information). [h]Disbonding prevented in experimental setup.

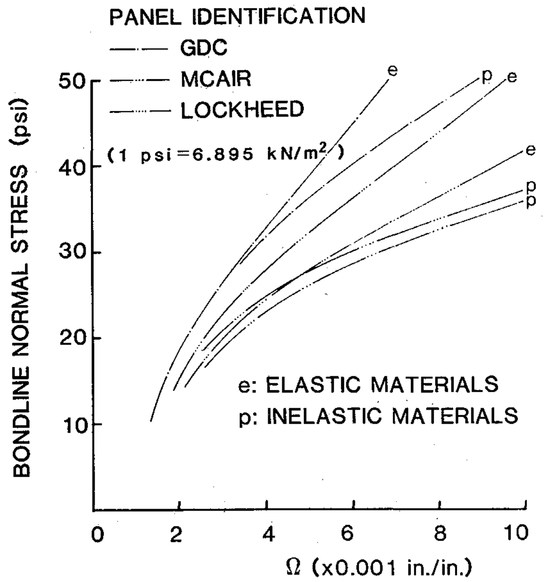

Fig. 8 Bondline normal stresses in edge-stiffened flat panels in shear.

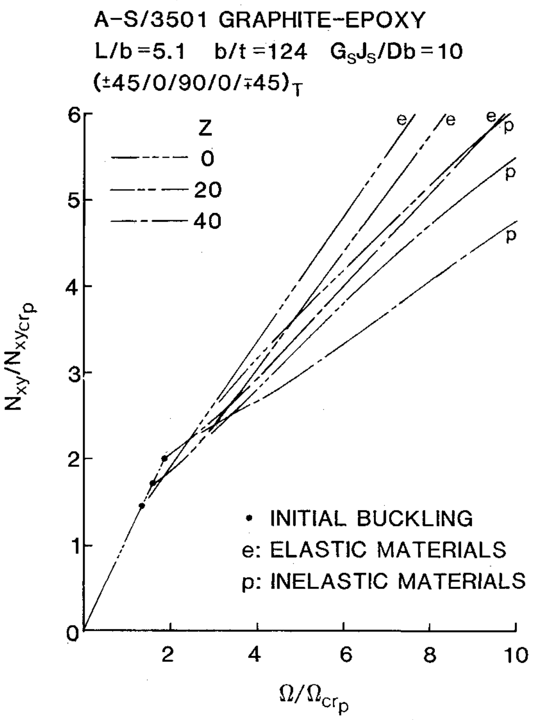

Fig. 9 Effect on curvature on the postbuckling behavior of edge-stiffened panels in shear.

Postbuckling of Curved, Stiffened Panels in Combined Compression and Shear

As metioned earlier, experimental load-deformation curves to failure for curved stiffened panels in combined compression and shear are not available at this time. To demonstrate the trends, several representative shear stress/strain curves are presented. The basic layup is that of the McAir test specimen. The important influences of curvature (Fig. 9), edge stiffening (Fig. 10), and boundary conditions (Fig. 11) are presented and discussed in order. Each figure shows the results of both an elastic and an inelastic material behavior assumption. Figure 9 presents the shear stress/strain curves for the McAir panel with the edges essentially clamped ($G_sJ_s/Db = 10$) for various values of the curvature parameter Z. It is observed that increasing the curvature parameter (that is, decreasing the radius) causes the initial buckling load to be higher; however, the postbuckling stiffness is reduced. Figure 10 illustrates the effect of edge stiffening on a curved panel. The essentially clamped panel ($G_sJ_s/Db = 10$) has a higher initial buckling load, but the postbuckling stiffness of each panel is essentially identical for $\Omega/\Omega_{cr} > 4$. The plate can have a multitude of different boundary conditions along the stiffened edges. Illustrated in Fig. 11 are two possible situations: the constrained boundary condition corresponding to the restriction that the y-direction edges are not allowed to move (thus causing circumferential tensile stresses to be developed during shear loading) and the unconstrained boundary condition that allows movement of the y-direction edges, but specifies the average circumferential stress to be zero. The effect of these boundary conditions, as depicted in Fig. 11, is quite substantial. Thus, for good correlation of both experimental data and analytical predictions, the actual boundary conditions must be accurately reflected in the analysis.

For combined loads, Fig. 12 shows the shear stress/strain curves for a curved stiffened panel for various values of applied end shortening (compression). Similarly, the load-shortening curve is shown for various values of applied shear as shown in Fig. 13. Figure 14 shows the maximum inward and outward displacements as a function of the applied shear load for various values of curvature and end shortening. Notice that for $Z = 0$ (flat panel), the inward and outward displacements are the same. However, as the curvature increases ($Z = 20$), the inward displacement increases and the outward displacement decreases, eventually reaching a zero value. The out-of-plane displacements for a combined loads case is also shown in Fig. 15. The mode shape of Fig. 14 is depicted in Fig. 15 for a curved, stiffened panel in shear.

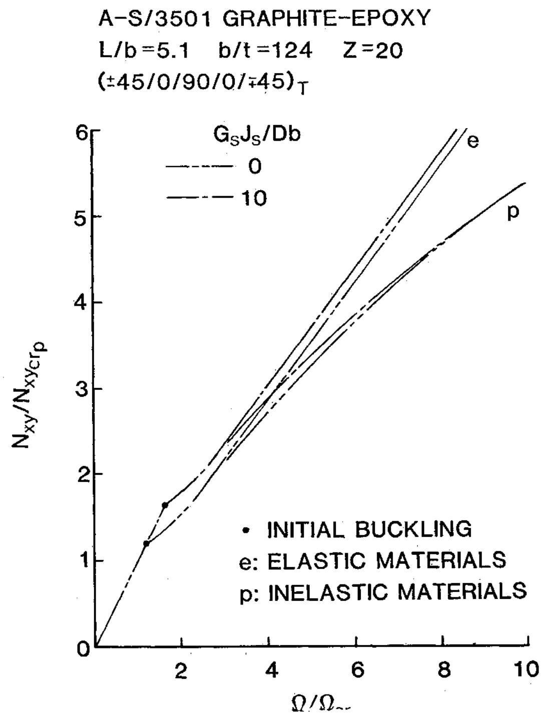

Fig. 10 Effect of edge stiffening on the postbuckling behavior of a curved panel in shear.

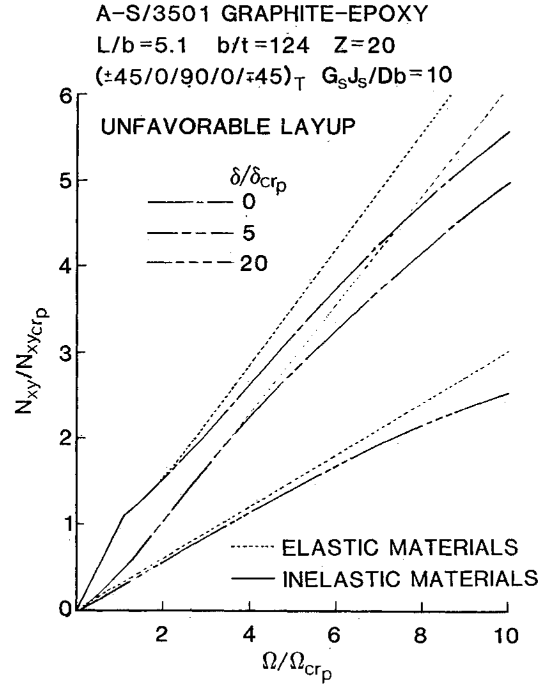

Fig. 12 Shear postbuckling behavior of an edge-stiffened curved panel under compression.

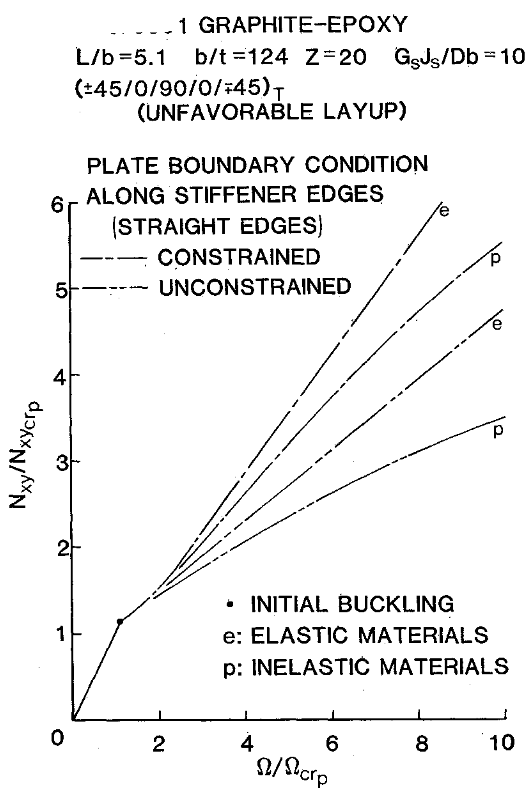

Fig. 11 Effect of boundary conditions on the postbuckling behavior of an edge-stiffened curved panel in shear.

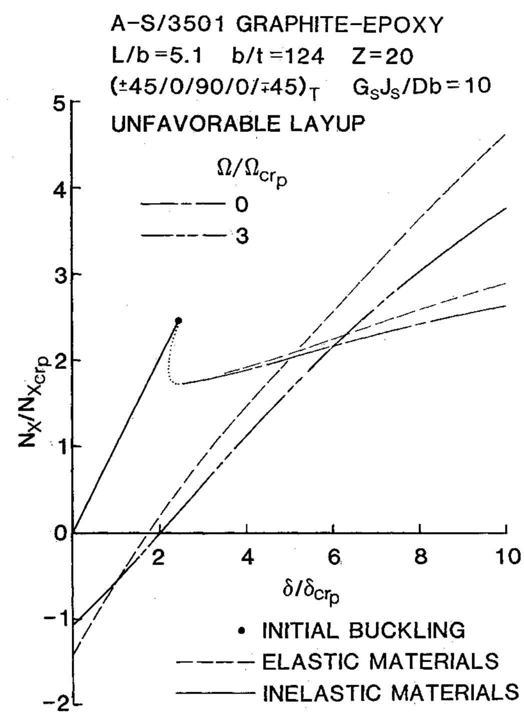

Fig. 13 Comparison of postbuckling behavior of an edge-stiffened curved panel under shear.

Prediction of Failure

The most common observed failure mode for composite panels is stiffener disbonding. However, there are other failure modes that may become important as the stiffener disbonding problem is solved: i.e., panel crippling due to exceeding the fiber strain allowables (either tension or compression), delamination due to excessive transverse or interlaminar stresses, and fatigue are all potential failure modes. It is important to note that the theory and analysis presented herein cannot predict failure by itself—failure can be predicted only by comparing the calculated stresses and strains to the appropriate allowable; subsequently, comparison to actual test data can demonstrate the applicability of the overall approach. The preceding parts of this paper have attempted to show that initial buckling and postbuckling behavior are accurately predictable using the present theory and assumed displacement and stress functions. Now, these calculated stresses and strains will be used to predict failure. This presentation is meant to be illustrative, inasmuch as a more comprehensive discussion of failure mechanisms is too lengthy to be included here and is thus postponed to a future paper.

Table 2 presents the correlation of predictions and experimental results for the four panels discussed earlier (GDC, Anamet, McAir, and Lockheed). To establish the predictions, the following procedure was utilized. For panel crippling, the fiber allowable strains were taken to be 1.1% in compression and 1.3% in tension. These strains represent reasonable design allowables for both AS/3501 and T300/5208 graphite/epoxy. Using Fig. 7, the applied shear strains corresponding to both tension and compression were determined. Knowing the applied shear strains and the load-shear strain curve, the shear load in the panel (stiffener not included) was determined and is documented in Table 2. For stiffener disbonding, the allowable normally directed bondline stress was taken to be 33 psi (227.5 kPa) based upon the pull-off specimen testing of Ref. 41. For final failure in the disbond failure mode, the allowable was arbitrarily chosen to be 36 psi (248.2 kPa), thus permitting comparison to the final panel failure. The procedure for determining the predicted load for stiffener disbonding is similar to that used for predicting panel crippling, except that Fig. 8 is required. Referring to Table 2, it is observed that in each case stiffener disbonding is the critical failure mode. This was also confirmed experimentally in each circumstance. Note that the experimental failure load for the panel is obtained by subtracting the estimated load taken by the stiffener/frame in shear from the total load determined experimentally. The stiffener/frame shear loads were obtained through a combination of finite-element analyses of the panel/frame assembly and hand calculations. The predicted and experimental loads for stiffener disbonding are in good agreement, as can be seen from Table 2. Given the fact that there is no doubt some variability in the bondline quality (and hence allowable normal stress), these comparisons are quite adequate. Also not to be overlooked is the fact that the predictions are based on design allowables; thus, it would be anticipated, indeed even required, that the predictions be below the actually demonstrated capability.

Another failure mode of some potential importance is delamination due to excessive interlaminar and transverse stresses. The various curves shown herein used an allowable transverse stress in the matrix of 3000 psi (20.7 MPa) in order to preserve the stability of the nonlinear material routines. Thus, if the transverse stress at a point was found to be in excess of 3000 psi (20.7 MPa), then that particular point was assumed to be damaged and only the elastic behavior was considered. This particular assumption applies only to the nonlinear material analysis. For flat plates, this limit on transverse shear stress has a minimal effect on the load shortening or shear stress/strain curves. However, for curved plates, the transverse shear stresses are relatively high. Thus, the nonlinear material curves must, at this time, be regarded as reasonable estimates of the effects of the nonlinear material assumption. Physically speaking, these calculated large transverse stresses indicate a potential practical limit on the curvature parameter Z. That is to say, if the panel is too highly curved, the presence of degrading transverse stresses may limit the static strength and fatigue life too drastically when compared to the initial buckling load. This particular failure mode will require further study and comparison to test data before a definitive statement can be made about the role of transverse shear stresses.

Conclusions

The design/analysis methodology for postbuckled panels described here is relatively complete in the sense that many important geometrical and material effects are included in the underlying theoretical foundation. The results, which include comparison to experimental data, provide the designer with a methodology that is mature and applicable to aircraft primary and secondary composite structures. Most importantly, the methodology is cost effective in that the extensive experimental programs required to develop reliable primary structures can usually be reduced in scope with an increased emphasis on computerized design.

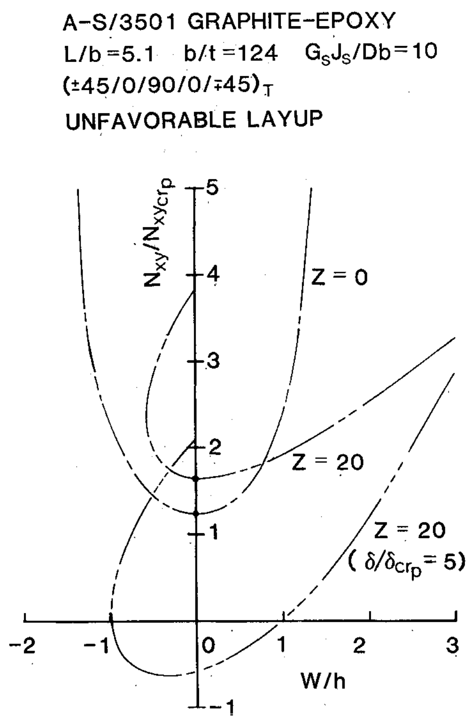

Fig. 14 Out-of-plane displacements for edge-stiffened panels with varying curvature and applied combined loads.

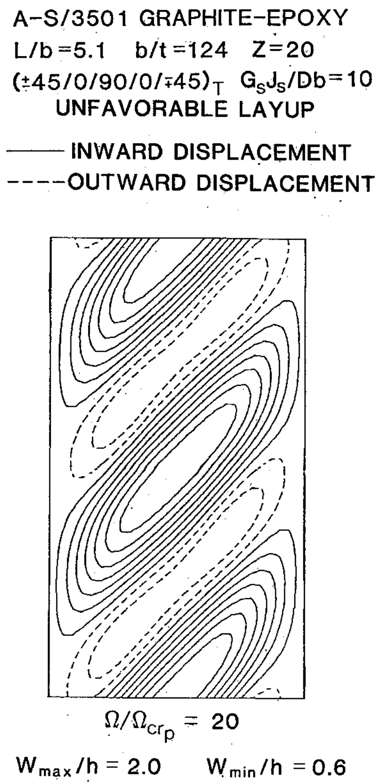

Fig. 15 Typical contour plot of out-of-plane displacements for an edge-stiffened curved panel in shear.

Acknowledgments

The authors would like to acknowledge the continuing encouragement and advice of Prof. (Emeritus) J. Mayers, Stanford University, Stanford, CA.

References

[1]Timoshenko, S., "Buckling of Rectangular Plates under the Action of Shearing Stresses," *Memoirs of the Institute of Engineers of Ways of Communication*, Vol. 89, 1915, p. 23.

[2]Timoshenko, S., *Theory of Elastic Stability*, 1st ed., McGraw-Hill, New York, 1936, p. 382.

[3]Southwell, R. V. and Skan, S. W., "On the Stability Under Shearing Forces of a Flat Elastic Strip," *Proceedings of the Royal Society of London*, Ser. A, Vol. 105, June 1924, pp. 582–607.

[4]Seydel, E., "Wrinkling of Reinforced Plates Subjected to Shear Stresses," translation from German by J. Vanier, NACA TM 602, 1931.

[5]Bergmann, St. and Reissner, H., "Buckling of Corrugated Strips Subjected to Shear Stresses," *Zeitschrift für Flugtechnik und Motorluftschiffahrt*, 1929, p. 475.

[6]Bollenrath, F., "Wrinkling Phenomena of Thin Flat Plates Subjected to Shear Stresses," translation from German by J. Vanier, NACA TN 601, Jan. 1931.

[7]Leggett, D. M. A., "The Elastic Stability of a Long and Lightly Bent Rectangular Plate Under Uniform Shear," *Proceedings of the Royal Society of London*, Ser. A, Vol. 162, No. 908, Sept. 1, 1937, pp. 62–83.

[8]Kromm, A., "The Limit of Stability of a Curved Plate Strip Under Shear and Axial Stresses," translated from German, NACA TM 898, June 1939.

[9]Stowell, E. Z. and Schwartz, E. B., "Critical Stress for an Infinitely Long Flat Plate with Elastically Restrained Edges under Combined Shear and Direct Stress," NACA WRL-340, 1943 (also ARR 3K13, Nov. 1943).

[10]Stowell, E. Z., "Critical Shear Stress of an Infinitely Long Flat Plate with Equal Elastic Restraints Against Rotation Along the Parallel Edges," NACA WRL-476, 1943 (also ARR 3K12, Nov. 1943).

[11]Batdorf, S. B. and Houbolt, J. C., "Critical Combinations of Shear and Transverse Direct Stress for an Infinitely Long Flat Plate with Edges Elastically Restrained Against Rotation," NACA Rept. 847, 1946.

[12]Stein, M. and Neff, J., "Buckling Stresses of Simply Supported Rectangular Flat Plates in Shear," NACA TN 1222, March 1947.

[13]Batdorf, S. B. and Stein, M., "Critical Combinations of Shear and Direct Stress for Simply Supported Rectangular Flat Plates," NACA TN 1223, March 1947.

[14]Batdorf, S. B., Schildcrout, M., and Stein, M., "Critical Shear Stress of Long Plates with Transverse Curvature," NACA TN 1346, June 1947.

[15]Batdorf, S. B., Schildcrout, M., and Stein, M., "Critical Combinations of Shear and Longitudinal Direct Stress for Long Plates with Transverse Curvature," NACA TN 1347, June 1947.

[16]Cox, H. L., "Summary of the Present State of Knowledge Regarding Sheet Metal Construction," British Aeronautical Research Council, L&M 1553, 1933.

[17]Iguchi, S., "Die Knickung der rechtechkigen Platte durch Schubkräfte," *Ingenieur-Archiv*, Bd. IX, Heft 1, Feb. 1938, pp. 1–12.

[18]Smith, R. C. T., "The Buckling of Plywood Plates in Shear," Div. of Aeronautics, Council for Science and Industry Research, Commonwealth of Australia, Rept. SM 51, Aug. 1945.

[19]Budiansky, B. and Connor, R. W., "Buckling Stresses of Clamped Rectangular Flat Plates in Shear," NACA TN 1559, May 1948.

[20]Budiansky, B. and Hu, P. C., "The Lagrangian Multiplier Method of Finding Upper and Lower Limits to Critical Stresses of Clamped Plates," NACA TN 1103, 1946.

[21]Schildcrout, M. and Stein, M., "Critical Combinations of Shear and Direct Axial Stress for Curved Rectangular Panels," NACA TN 1928, Aug. 1949.

[22]Gerard, G. and Becker, H., "Handbook of Structural Stability—Part III, Buckling of Curved Plates and Shells," NACA TN 3781, July 1957.

[23]Bruhn, E. F., "Analysis and Design of Flight Vehicle Structures," Jacobs and Associates, Indianapolis, IN, June 1973.

[24]Stein, M. and Fralich, R. W., "Critical Shear Stress of Infinitely Long, Simply Supported Plate with Transverse Stiffeners," NACA TN 1851, April 1949.

[25]Rockey, K. C. and Cook, I. T., "Influence of Torsional Rigidity of Transverse Stiffeners Upon the Shear Buckling of Stiffened Plates," *The Aeronautical Quarterly*, Vol. XX, May 1964, pp. 198–202.

[26]Lekhnitskii, S. G., *Anisotropic Plates*, 2nd ed., translated from Russian by S. W. Tsai and T. Cheron, Gordon & Breach Science Publishers, Baltimore, 1984.

[27]Balabukh, L. I., "Stability of Plywood Plates," *Tekhnika Vozdushnogo Flota*, No. 9, 1937.

[28]Viswanathan, A. V., Tamekuni, M., and Baker, L. L., "Elastic Stability of Laminated, Flat and Curved Long Rectangular Plates Subjected to Combined Inplane Loads," NASA CR-2330, June 1974.

[29]Sawyer, J. W., "Flutter and Buckling of General Laminated Plates," *Journal of Aircraft*, Vol. 14, April 1977.

[30]Zhang, Y. and Matthews, F. L., "Initial Buckling of Curved Panels of Generally Layered Composite Materials," *Composite Structures*, Vol. 1, June 1983, pp. 3–30.

[31]Whitney, J. M., "Buckling of Anisotropic Laminated Cylindrical Plates," *AIAA Journal*, Vol. 22, Nov. 1984, pp. 1641–1645.

[32]Leissa, A. W., "Buckling of Laminated Composite Plates and Shell Panels," AFWAL-TR-85-3069, June 1985, p. 454.

[33]Bouadi, H., "Buckling and Postbuckling of Composite Plates," Engineer's Thesis, Stanford University, Stanford, CA, Aug. 1982.

[34]Giaedi, A. A., "On Buckling and Postbuckling of Composite Square Plates in Shear," Engineer's Thesis, Stanford University, Stanford, CA, Sept. 1983.

[35]Feng, M., "An Energy Theory for Postbuckling of Composite Plates Under Combined Loading," *Computers & Structures*, Vol. 16, No. 1–4, 1983, pp. 423–431.

[36]Stein, M., "Postbuckling of Long Orthotropic Plates in Combined Shear and Compression," AIAA Paper 83-0876, 1983.

[37]Zhang, Y. and Matthews, F. L., "Postbuckling Behavior of Anisotropic Laminated Plates under Pure Shear and Shear Combined with Compressive Loading," *AIAA Journal*, Vol. 22, Feb. 1984, pp. 281–286.

[38]Kaminski, B. E. and Ashton, J. E., "Diagonal Tension Behavior of Boron-Epoxy Shear Panel, *Journal of Composite Materials*, Vol. 5, Oct. 1971, pp. 553–558.

[39]Kobayashi, S., Sumihara, K., and Koyama, K., "Shear Buckling Strength of Graphite-Epoxy Laminated Panels," *Composite Materials, Proceedings of Japan-U.S. Conference*, Tokyo, 1981.

[40]Schneider, G. J., "Initial Buckling and Diagonal Tension Behavior of Kevlar/Graphite Epoxy Flat Stiffened Shear Panels," Sikorsky Aircraft, Rept. SER-510047, prepared for Naval Air Systems Command, April 1981.

[41]Ostrom, R. B., "Post-Buckling Fatigue Behavior of Flat, Stiffened Graphite/Epoxy Panels Under Shear Loading," NADC-78137-60, May 1981.

[42]Sumihara, K., Kobayashi, S., and Koyama, K., "Shear Buckling Strength of CFRP Laminated Panels (1st Report)," *Journal of the Japan Society for Aeronautical and Space Science*, Vol. 29, June 1981, pp. 321–332.

[43]Reneiri, M. P. and Garrett, R. A., "Postbuckling Fatigue Behavior of Flat Stiffened Graphite/Epoxy Panels Under Shear Loading," NADC-78137-60, Aug. 1980.

[44]Bear, K. R., "Shear Testing of a GD/Convair IRAD Composite Adaptor Panel," McDonnell Aircraft Co., TM 253.4225, Feb. 2, 1984.

[45]Yoo, S. Y., "On Maximum Strength of Plates Under Axial Compression—Effects of Curvature and Edge-Stiffener Extensional and Torsional Rigidity," Ph.D. Dissertation, Stanford University, Stanford, CA, 1977.

[46]Anderson, R. E. and Mayers, J., "Effects of Non-linear Material Behavior on Postbuckling Stiffness of Laminated Composite Plates," AIAA Paper 79-1806, Aug. 1979.

[47]Arnold, R. R. and Mayers, J., "Buckling, Postbuckling and Crippling of Materially Nonlinear Laminated Composite Plates," *International Journal of Solids and Structures*, Vol. 20, 1984, pp. 863–880.

[48]Arnold, R. R., Yoo, S. Y., and Mayers, J., "Buckling, Postbuckling and Crippling of Shallow Curved Composite Plates with Edge Stiffeners," AIAA Paper 85-0769, 1985.

[49]Reissner, E., "On a Variational Theorem in Elasticity," *Journal of Mathematics and Physics*, Vol. XXIV, No. 2, July 1950, pp. 90–95.

[50]Arnold, R. R., "Buckling, Postbuckling, and Crippling of Materially Nonlinear Laminated Composite Plates," Ph.D. Dissertation, Stanford University, Stanford, CA, March 1983.